Downregulation of fascin induces collective cell migration in triple-negative breast cancer

YUMIKO YAMAMOTO[1], YOSHIHIRO HAYASHI[2,3], HIDEYUKI SAKAKI[4] and ICHIRO MURAKAMI[1,3]

[1]Department of Diagnostic Pathology, Kochi University Hospital, Kochi University; [2]Equipment of Support Planning Office, Kochi University; [3]Department of Pathology, School of Medicine, Kochi University, Kohasu, Nankoku, Kochi 783-8505; [4]Department of Nutritional Sciences for Wellbeing, Kansai University of Welfare Sciences, Kashiwara, Osaka 582-0026, Japan

Received December 2, 2022; Accepted April 20, 2023

DOI: 10.3892/or.2023.8587

Abstract. Breast cancer (BC) is one of the most common types of cancer affecting female patients. Triple-negative BC (TNBC) is an aggressive subtype. Fascin, an actin-bundling protein, serves a significant role in cancer metastasis. Fascin overexpression is associated with poor prognosis of BC. To confirm the relationship between fascin expression and BC malignancy, the present study reviewed clinical data from 100 Japanese patients with BC and performed fresh immunohistochemical fascin examination of tissue samples. Statistical analyses showed metastasis or recurrence in 11 of 100 patients and a significant association between high fascin expression and poor prognosis. The TNBC subtype was also associated with high fascin expression. However, a few cases developed poor prognosis regardless of negative or slightly positive fascin expression. The present study established fascin knockdown (FKD) MDA-MB-231, a TNBC cell line, and investigated morphological effects of fascin on TNBC cells. FKD cells exhibited cell-cell connections and bulbous nodules of various sizes on the cell surface. Conversely, non-FKD MDA-MB-231 cells exhibited loose cell-cell connections with numerous filopodia on the cell surface. Filopodia, actin-rich plasma membrane protrusions, are composed of fascin and control cell-cell interaction, migration and wound healing. Cancer metastasis is conventionally classified into two mechanisms: single and collective cell migration. Fascin increases cancer metastasis by single cell migration via filopodia on the cell surface. However, the present study suggested that following FKD, TNBC cells lost filopodia and exhibited collective cell migration.

Correspondence to: Dr Yumiko Yamamoto, Department of Diagnostic Pathology, Kochi University Hospital, Kochi University, 185-1, Kohasu, Oko-cho, Nankoku, Kochi 783-8505, Japan
E-mail: jm-yumikoyamamoto@kochi-u.ac.jp

Key words: fascin, triple-negative breast cancer, collective cell migration, single cell migration, wound healing assay, spheroid

Introduction

Breast cancer (BC) is one of the most common types of cancer affecting women (1-3) and the number of patients diagnosed with BC remains high worldwide as indicated in the WHO data up to 2016 (1). In Japan, BC is the most frequently diagnosed cancer in women (4). However, recent reports present that mortality rates of BC tend to decrease especially in developed countries (1,2), which could be attributed to the progress of diagnostic methods and therapies for BC (1-5). Despite advances in BC research and treatment, due to the lack of therapeutic targets, triple-negative BC (TNBC) is regarded as an aggressive subtype with a poor prognosis and its clinical outcome remain, unsatisfactory (1,6,7).

Fascin, an actin-bundling protein, serves a significant role in the regulation of cell adhesion, migration, and invasion (8-15). Fascin is strongly upregulated in several types of human carcinoma and sarcoma (8-12,14). Fascin overexpression is associated with higher grade of BC and its expression commonly predicts an aggressive clinical course in patients (7,10,13,16,17). Filopodia, bundles of actin, are fibrous protrusions on the cell membrane. They are also essential in processes of cell proliferation, including adhesion, migration and the formation of cell-cell contacts. Filopodia allow cells to migrate to the surrounding tissue through the extracellular matrix by interacting with various types of intercellular adhesive structure such as tight junctions, adherens junctions containing cadherin and desmosomes (18).

The present study reviewed clinical data from 100 patients diagnosed with BC in 2015. Fresh immunohistochemical assessment of fascin in tissue samples was performed to examine the association between BC malignancy with fascin expression and TNBC subtype. The present study aimed to investigate the association between fascin and BC invasion by morphological observation of cytoplasm and the cell surface. Fascin knockdown (FKD) was induced in MDA-MB-231, a TNBC cell line, to detect morphological effects of fascin on TNBC cells.

Materials and methods

Clinical data of patients with BC. Clinical data were reviewed from 100 consecutive patients who had been diagnosed with

early-stage BC at Kochi University Hospital, Nankoku, Japan, from January to December 2015. The study was reviewed and approved by the Ethic Committee for Clinical Research of the School of Medicine, Kochi University (approval no. 2020-123; 4th December 2020). Written consent to participate was obtained from all patients. All 100 patients had undergone surgical treatment and completed follow-up for >5 years at the hospital. All tissues obtained during surgery had been embedded in paraffin blocks following formalin fixation for preservation. The immunohistochemical evaluation of estrogen receptor (ER), progesterone receptor (PR) and human epidermal growth factor receptor 2 (HER2) were also reviewed from clinical pathology reports at the time of initial diagnoses.

Fascin immunohistochemical evaluation. A total of 11 tissue samples from patients with metastasis or recurrence during 5-year follow-up were cut into 4 μm thick slices and heat-treated at 95˚C for 30 min with ULTRA cell conditioning 1 retrieval solution (Ventana Automated Systems). Immunohistochemical examination was performed using a Ventana automated system with anti-fascin-1 mouse monoclonal antibody (1:100; cat. no. M3567; Dako, Agilent Technologies, Inc.). Another set of 17 consecutive tissue samples from patients without metastasis or recurrence underwent the same procedure as a control group. To evaluate immunohistochemical expression of fascin, the Allred scoring system was used (13,14). Briefly, the proportion of stained cells was categorized as negative (0), <1 (1), 1-10 (2), 11-33 (3), 34-66 (4) and >66% (5) positive. The intensity of the most predominantly stained area was categorized as no (0), weak (1), intermediate (2), or strong (3) staining (Fig. 1). Allred score (0-8 points) was calculated by adding the proportion and intensity values. Independent evaluation of immunostaining was performed by two expert pathologists (YH, IM).

FKD MDA-MB-231 cells. Human TNBC MDA-MB-231 cells (American Type Culture Collection), were cultured at 37˚C for 24 h with 5% CO_2 in DMEM (Sigma-Akdrech, Merck KGaA) with 10% fetal bovine serum (Biosera France SAS). Following recombination of the short hairpin RNA (shRNA) against fascin, the pLKO.1-puro plasmid vector (1 μg/μl; Clone ID: NM_003088.2-1699s1c; Sigma-Aldrich, Merck KGaA), containing the puromycin-resistance gene, was transfected into MDA-MB-231 cells with FuGene®6 Transfection Reagent (Roche Diagnostics) at 37˚C for 24 h, according to the manufacturer's instructions. Cells were incubated at 37˚C with 2.2 μg/ml puromycin (Sigma-Akdrech, Merck KGaA) for 2 weeks. Puromycin-resistant colonies (~20) were obtained and cultured with the medium containing puromycin (2.2 μg/ml) in 100 mm-diameter dishes. When the cell confluency reached 80%, dishes were provided to carry out western blot analysis and to gain FKD MDA-MB-231 cells, respectively. Transfection of the pLKO.1-puro plasmid vector without shRNA against fascin was used to generate non-FKD MDA-MB-231 cells.

Immunocytochemical and phalloidin staining of MDA-MB-231 cells. For immunocytochemical staining, non-FKD and FKD MDA-MB-231 cells were incubated with anti-fascin-1 mouse monoclonal antibody (1:100; cat. no. M3567; Dako, Agilent Technologies, Inc.) at 4˚C overnight reacted with fluorescein isothiocyanate (FITC)-labeled anti-mouse IgG antibody (1:200; cat. no. F-2761; Molecular Probes, Thermo Scientific, Inc.) at room temperature for 1 h and nuclei were stained with DAPI (Sigma-Akdrech, Merck KGaA). For phalloidin staining, cells ($2x10^4$/well) were cultured at 37˚C for 24 h on a slide chamber (AGC Techno Co., Ltd), fixed with 100% acetone at -20˚C for 20 min and stained with FITC-labeled phalloidin (Sigma-Akdrech, Merck KGaA) to bind actin filaments, according to the manufacturer's instructions. Fluorescence microscopy was performed using an Olympus BX53 (Olympus Corporation; magnification x200) with cellSens standard (ver.1.12, Olympus Corporation).

Western blot analysis. Concentration of samples lysed in RIPA Buffer (Fujifilm Wako Pure Chemical Corp) was measured by Pierce BCA Protein Assay Kit (cat. no. 23227; Thermo Fisher Scientific, Inc.). 20 μg/lane samples were prepared for SDS-PAGE separation (10% SDS-PAGE Gel; Bio-Rad Laboratories, Inc.) and transferred to polyvinylidene difluoride membranes using the Trans-Blot Turbo Transfer System (Bio-Rad Laboratories, Inc.). Membranes were blocked with Blocking One (cat. no. 03953-93; Nacalai Tesque, Inc.) at room temperature for 1 h, and incubated at 4˚C overnight with following antibodies: anti-fascin-1 mouse monoclonal (1:500; cat. no. M3567; Dako, Agilent Technologies, Inc.), E-cadherin mouse monoclonal (1:500; cat. no. M3612; Dako, Agilent Technologies, Inc.), Snail1 rabbit polyclonal antibody (1:200; cat. no. Ap205Aa; Adgent, Inc.), and GAPDH mouse monoclonal antibody (1:2000; cat. no. 20035; ProMab Biotechnologies, Inc.). Then, the membranes were incubated at room temperature for 1 h with either of following secondary antibodies: HRP-labeled anti-mouse polyclonal antibody (1:2000; cat. no. P0447; Dako, Agilent Technologies, Inc.) or anti-rabbit polyclonal antibody (1:2000; cat. no. P0399; Dako, Agilent Technologies, Inc.). Bands were visualized by ECL Prime Western Blotting Detection Reagents (Amersham, Cytiva) and observed using LAS-4000 Lumino-Image Analyzer (FUJIFILM Wako Pure Chemical Corporation). ImageJ (version no. 1.53; National Institutes of Health) was used for analysis.

Wound healing assay. Trypsinized $2x10^4$/ml parent, non-FKD and FKD cells were counted with SKC, Inc. C-Chip™ Disposable (Thermo Fisher Scientific), disposable hemocytometer, seeded onto a 35 mm-diameter dish and cultured at 37˚C for 48 h. When the cell confluence reached 90%, a scratch was made through the center of the cell layer using a 20-μl pipette tip. The cells were incubated using 10% FBS at 37˚C for 20 h. Phase-contrast microscopy was performed at 0, 12, 16 and 20 h on 50 spots, which were randomly marked on 35-mm dishes containing each cell (Olympus Corporation, CKX41, original magnification x200). To investigate cell migration ratio, the area of each scratch without cell migration was measured in the same size dimension with the same magnification, using ImageJ software, ver.1.53. The mean migration of 50 spots in each cell sheet was examined. Then, the mean value at 0 h was defined as 1.0 and relative cell migration ratio was detected at each time of each cell.

Correlative light and electron microscopy (CLEM). As aforementioned, a scratch was made using a 20-μl pipette tip on a layer

Table I. Reagents and suppliers.

Reagent	Supplier	Dilution
Anti-fascin-1 mouse monoclonal antibody	Dako (Agilent Technologies, Inc.)	1:100
Anti-vimentin mouse monoclonal antibody	Dako (Agilent Technologies, Inc.)	1:200
Anti-E-cadherin mouse monoclonal antibody	Dako (Agilent Technologies, Inc.)	1:100
Anti-Snail1 rabbit polyclonal antibody	Abgent, Inc.	1:100
Anti-GAPDH mouse monoclonal antibody	ProMab Biotechnologies, Inc.	1:2,000
Biotinylated goat anti-rabbit IgG antibody	Abcam	1:200
Biotinylated rabbit anti-mouse IgG antibody	Dako (Agilent Technologies, Inc.)	1:200
FITC-labeled streptavidin	Dako (Agilent Technologies, Inc.)	1:200
Texas Red-labeled anti-rabbit IgG antibody	Molecular Probes (Thermo Fisher Scientific, Inc.)	1:200
N-Histofine Simple Stain MAX PO (MULTI)	Nichirei Biosciences Inc.	Ready to use
DAB	Sigma Aldrich (Merck KGaA)	Tablet/15 ml distilled water

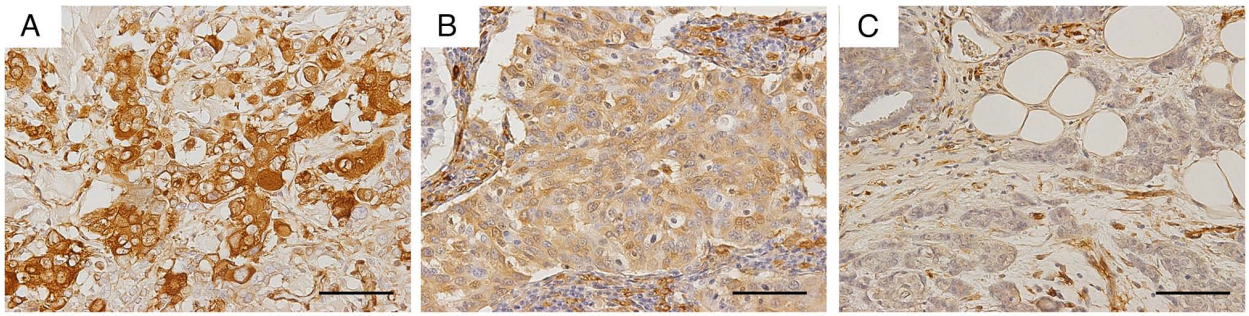

Figure 1. Fascin immunohistochemical expression in tissue from patients with breast cancer. Representative images of (A) strong, (B) intermediate and (C) weak fascin expression. The tissue samples were from Cases 7, 14 and 8, respectively. Scale bar, 50 μm.

of non-FKD and FKD cells ($2x10^4$/well each) seeded onto the slide chambers (AGC Techno Co., Ltd). Immunocytochemical staining with anti-fascin-1 mouse monoclonal antibody and FITC-labeled anti-mouse IgG antibody was performed as aforementioned. Following immunofluorescence microscopy, cells were fixed with 2.5% glutaraldehyde and 1% osmic acid at 4˚C for 6 h and 1h, respectively. Then, cells were stained with 1% phosphotungstic acid at room temperature for 10 min and low-vacuum scanning electron microscopy (LV-SEM) was performed. Finally, images of immunofluorescence and LV-SEM were superimposed using ImageJ software, ver.1.53.

Hematoxylin-eosin (HE) and immunohistochemical stain of non-FKD and FKD MDA-MB-231 cells cultured in Cellmatrix®. A total of $1x10^4$/ml non-FKD and FKD MDA-MB-231 cells were counted as aforementioned and Cellmatrix (Nitta Gelatin Inc.) was prepared according to the manufacturer's instructions. Subsequently, each group of cells and 500 μl Cellmatrix® were poured into a 35-mm-diameter dish (coated with Cellmatrix at 37˚C for 30 min), covered with 200 μl DMEM and cultured at 37˚C for 10 days. The gels were fixed in 20% buffered formaldehyde at room temperature overnight and embedded in paraffin. Following HE stain (Mayer's hematoxylin and 1% eosin staining at room temperature for 10 and 5 min, respectively), immunohistochemical staining for E-cadherin, Snail1 and vimentin was performed as follows. 4 μm-thick tissue samples were immersed in 0.01 M citrate buffer (pH 7.0) for antigen retrieval (98˚C, 30 min). Sections were immersed in 0.3% hydrogen peroxide/methanol at room temperature for 10 min to remove endogenous peroxidase. Then, the sections were blocked using Blocking One (cat. no. 03953-93; Nacalai Tesque, Inc.) at room temperature for 1 h and incubated at 4˚C overnight with following antibodies: anti-E-cadherin mouse monoclonal antibody (1:100; cat. no. M3612; Dako, Agilent Technologies, Inc.), Snail1 rabbit polyclonal antibody (1:100; cat. no. Ap2054a; Adbent, Inc.) and vimentin mouse monoclonal antibody (1:200; cat. no. M725; Dako, Agilent Technologies, Inc.). After washing with PBS, sections were incubated in N-Histofine Simple Stain MAX PO (MULTI; cat. no. 424151; Nichirei Biosciences Inc.) at room temperature for 1 h and washed again with PBS. Finally, the sections were immersed in DAB substrate solution (tablet/15 ml distilled water; SIGMAFAST 3,3'-Diaminobenzin tablets; D4418; Sigma-Aldrich, Merck KGaA) and the nucleus was stained with Mayer Hematoxylin at room temperature for 1 min. Optical microscope images were performed using an Olympus BX53 with cellSens (Olympus Corporation). An additional set of gels was fixed in 2.5% glutaraldehyde at 4˚C for 6 h for LV-SEM.

Spheroids of non-FKD and FKD MDA-MB-231 cells. A total of $1x10^4$/well parent, non-FKD and FKD MDA-MB-231

Table II. Clinical data of patients with breast cancer.

Case	Age, years	Metastasis or recurrence	Hormone receptor status			Fascin expression		
			ER	PgR	HER2	Proportion	Intensity	Allred score
1	71	+	-	-	-	5	3	8
2	57	+	+	+	-	0	0	0
3	63	+	+	+	-	2	1	3
4	42	+	+	+	-	5	1	6
5	65	+	+	-	-	2	1	3
6	51	+	-	-	-	1	1	2
7	65	+	-	-	-	3	3	6
8	74	+	+	+	-	3	1	4
9	53	+	+	+	-	2	1	3
10	74	+	+	-	-	2	2	4
11	77	+	-	-	-	3	1	4
12	60	-	+	+	-	0	0	0
13	64	-	+	+	-	0	0	0
14	59	-	+	-	-	4	2	6
15	40	-	+	+	-	2	1	3
16	58	-	+	+	-	0	0	0
17	71	-	+	+	-	0	0	0
18	59	-	+	-	-	0	0	0
19	69	-	+	+	-	0	0	0
20	85	-	+	+	-	0	0	0
21	57	-	+	+	-	2	1	3
22	71	-	-	-	-	5	3	8
23	60	-	+	+	-	0	0	0
24	69	-	+	+	-	2	2	4
25	65	-	+	+	-	0	0	0
26	64	-	+	+	-	0	0	0
27	61	-	+	+	-	0	0	0
28	40	-	+	+	-	2	2	4

-, negative; +, positive; ER, estrogen receptor; PgR, progesterone receptor; HER2, human epidermal growth factor receptor 2.

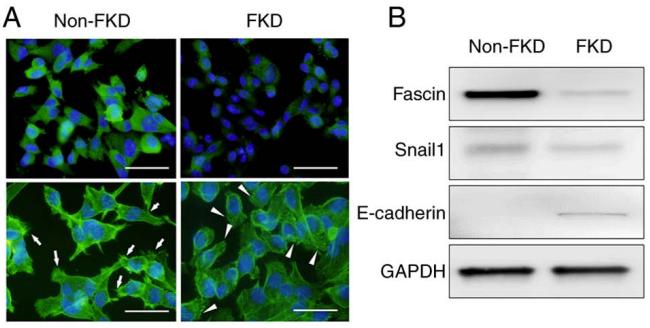

Figure 2. Establishment of FKD MDA-MB-231 cells. (A) Expression of Fascin (green) was strongly positive in non-FKD cells and effectively suppressed in FKD cells. Numerous filopodia, including actin filaments (arrows), were observed on the membrane of non-FKD cells, however, these filopodia decreased and actin-positive granules were detected (arrowheads) on the membrane of FKD cells. The cell nucleus was stained blue by DAPI in all pictures. Scale bar, 50 μm. (B) Western blot analysis of non-FKD and FKD cells. GAPDH was used as a control. FKD, fascin knockdown.

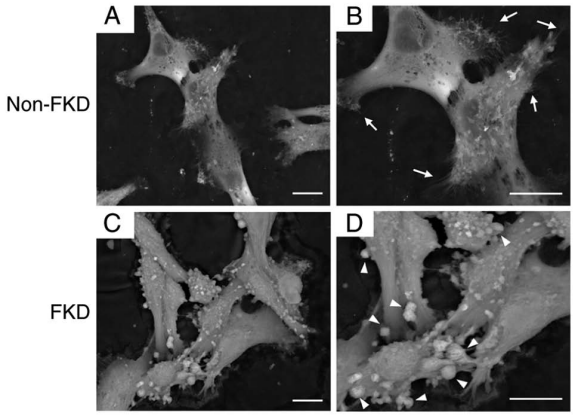

Figure 3. Two-dimensional low vacuum-scanning electron microscopy of non-FKD and FKD MDA-MB-231 cells. (A) Non-FKD cells exhibited loose cell-cell adhesion. (B) Bundles of extremely thin microfibrils (filopodia; arrows) on the cell surface. (C) FKD cells exhibited cell-cell adhesion. (D) Granular nodules (arrowheads) of various sizes on the cell surface. Scale bar, 10 μm. FKD, fascin knockdown.

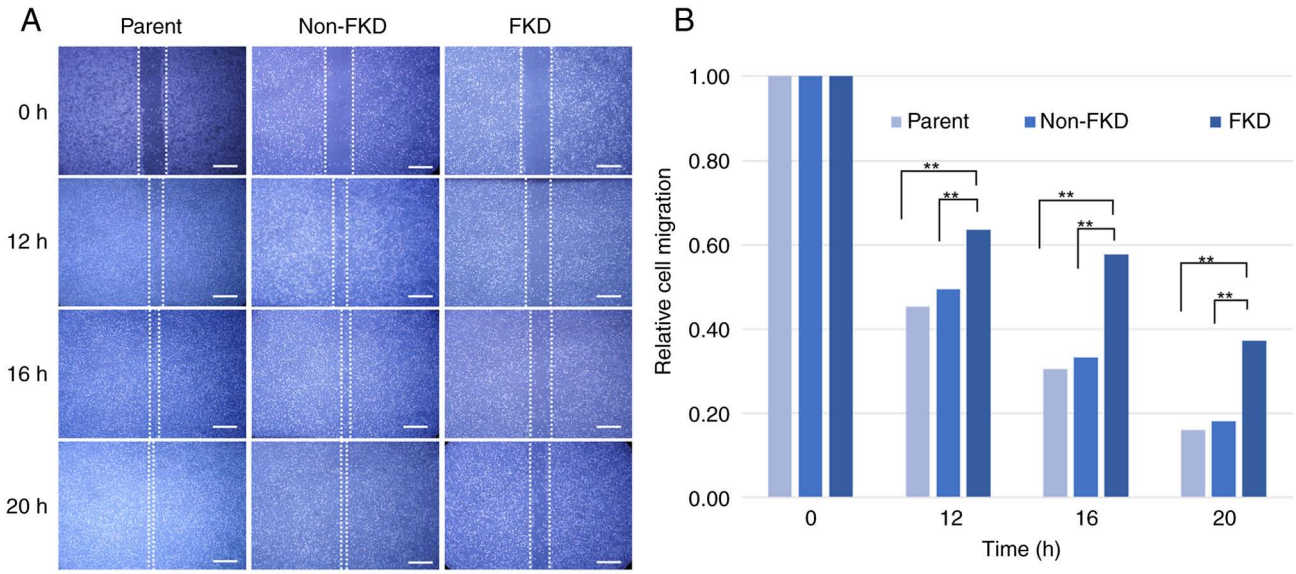

Figure 4. Wound healing assay of parent, non-FKD and FKD MDA-MB-231 cells. (A) Representative phase-contrast micrographs of wound healing assay. (B) Mean of relative cell migration at each time (n=50 for each group). The dynamics of FKD cell migration showed a statistical difference from parent and non-FKD cell migration. **P<0.01, Scale bar, 500 μm. FKD, fascin knockdown.

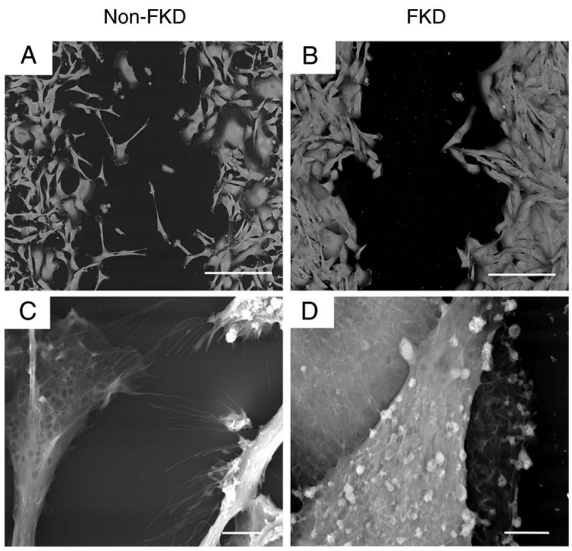

Figure 5. Two-dimensional low vacuum-scanning electron microscopy of wound healing assay of non-FKD and FKD MDA-MB-231 cells. (A) Non-FKD cells exhibited loose cell-cell connections. (B) FKD cells were observed as groups with tight cell-cell connections. Scale bar, 200 μm. (C) Bundles of extremely thin microfibrils (filopodia) were observed on the surface of leading migratory non-FKD cells. Scale bar, 5 μm. (D) Globular-shaped lamps of different sizes were observed on the surface of FKD cells. Scale bar, 10 μm. FKD, fascin knockdown.

cells were counted as aforementioned and seeded onto PrimeSurface® (Sumitomo Bakelite Co., Ltd.), 96-well plate with ultra-low adhesion round bottom dishes. Following incubation at 37˚C with 5% CO_2 for 5 days, multicellular spheroids were generated. As aforementioned, fixation of the samples, HE and immunohistochemical staining of fascin and E-cadherin for microscopy (Olympus BX53), and LV-SEM were completed. A total of 10 spheroids was collected in a 35-mm-diameter dish (coated with Cellmatrix at 37˚C for 30 min) with 500 μl Cellmatrix, covered with 200 μl DMEM and cultured at 37˚C for 3 days. After fixation in 20% buffered formaldehyde at room temperature for 6 h, the samples were observed under stereoscopic microscope MZ16FA (Leica Microsystems Tokyo, Japan, original magnification x200).

Immunohistochemistry of non-FKD and FKD MDA-MB-231. Immunohistochemical and immunofluorescent analyses were performed as previously described (9). The antibodies and chemical agents are shown in Table I.

LV-SEM. Samples containing cells or spheroids were fixed using 2.5% glutaraldehyde in 0.1M phosphate buffer (PB, pH 7.4) at 4˚C for 4 h and postfixed with 1% osmium tetroxide in PB at 4˚C for 1 h. Then, each block was washed with distilled water for 30 min and stained with 1% phosphotungstic acid solution at room temperature for 10 min. Following a final wash with distilled water for 30 min, the block was dried on an electrically conductive tape (Nisshin EM Co., Ltd.) and observed using a Miniscope® TM3030 (Hitachi Ltd.).

Statistical analysis. χ^2 test was performed to detect the association between a TNBC subtype and the incidence of metastasis or recurrence. Cochran-Armitage test was performed to detect the relationship between the Allred score and the incidence of metastasis or recurrence. χ^2 test was performed to analyze the relationship between E-cadherin expression in FKD and non-FKD cells, and Snail1 expression as well. Tukey-Kramer test was used to compare the mean values of cell migration ratios in wound healing assay. Two-side test was applied for all analyses except Cochran-Armitage test. JMP (ver. 14.3.0, SAS Institute inc.) was used for statistical analyses.

Results

Clinical data of patients with BC patients. A total of 11 out of 100 consecutive patients with BC developed metastasis or

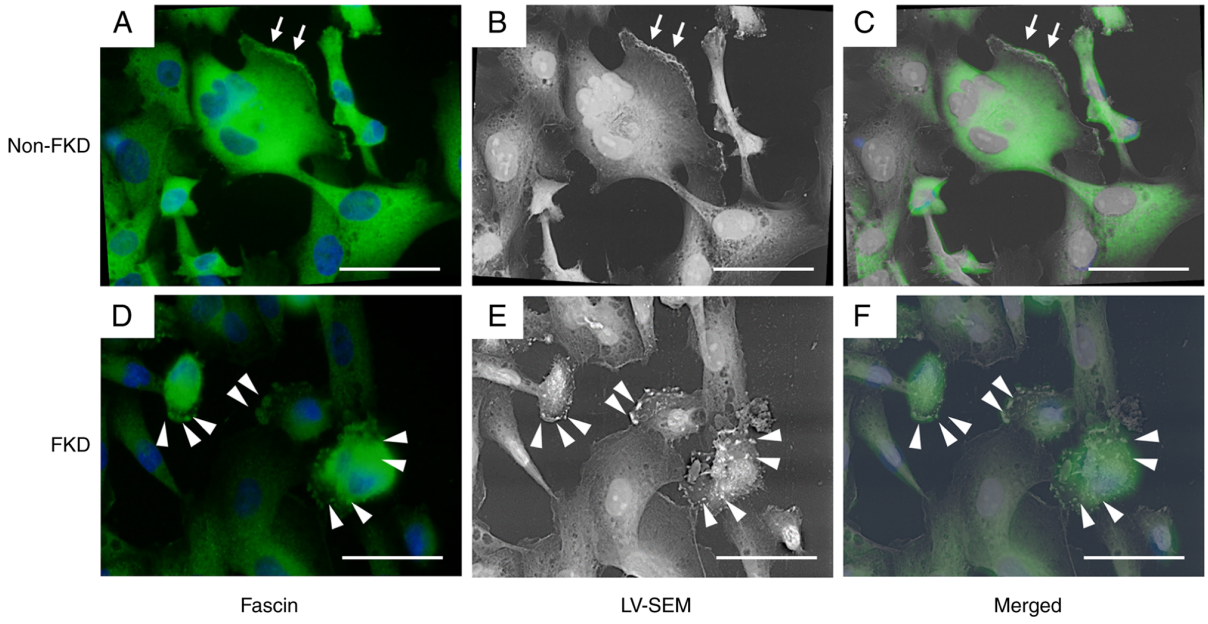

Figure 6. Correlative light and electron microscopy of leading migratory cells. (A) Fascin immunohistochemistry of non-FKD cells. Expression of fascin (green) was strongly positive. Arrows show the cell membrane with strong fascin experesion. The cell nucleus was stained in blue by DAPI. (B) Two-dimensional LV-SEM of non-FKD cells. Arrows show filopodia on the cell membrane. (C) Merged image. (D) Fascin immunohistochemistry of FKD cells. Expression of fascin (green) was effectively suppressed. Arrowheads show fascin-positive area on the cell membrane. The cell nucleus was stained in blue by DAPI. (E) Two-dimensional LV-SEM of FKD cells. Arrowheads show globular-shaped lamps observed on the cell membrane. (F) Merged image. Scale bar, 500 μm. FKD, Fascin knockdown; LV-SEM, low vacuum-scanning electron microscopy.

recurrence within five years (Table II). Fresh fascin immunostaining was performed on tissue samples from these patients as well as 17 patients without metastasis or recurrence. χ^2 test result showed a significant association between TNBC subtype and the incidence of metastasis or recurrence ($P<0.05$, Table II). Cochran-Armitage test showed a significant association between the Allred score of fascin and the incidence of metastasis or recurrence ($P<0.05$, Table II). However, Cases #2 and #6 developed poor prognosis regardless of negative or slightly positive fascin expression (0 and 2, respectively). Cases #14 and #22 did not develop metastasis or recurrence during follow-up periods, although they showed high Allred scores (6 and 8, respectively).

Establishment of FKD MDA-MB-231 cells. The expression of fascin (green) was strongly positive in non-FKD cells and effectively suppressed in FKD cells (Fig. 2A). Numerous filopodia, including actin filaments (arrows), were observed on the membrane of non-FKD cells, however, these filopodia were decreased and actin positive granules (arrowheads) were observed on the membrane of FKD cells. Fascin was strongly positive in non-FKD cells and was suppressed in FKD cells (Fig. 2B). Snail1 expression was also decreased in FKD cells. By contrast, E-cadherin expression increased in FKD cells.

2D LV-SEM were performed following 3 day cultivation of non-FKD and FKD MDA-MB-231 cells. Non-FKD cells exhibited loose cell-cell connections (Fig. 3A), however, bundles of extremely thin microfibrils on the cell surface were observed (arrows; Fig. 3B). FKD cells exhibited cell-cell adhesion (Fig. 3C) and granular nodules of various sizes were observed on the cell surface (arrowheads; Fig. 3D).

Wound healing assay. Following 20 h incubation, the mean scratch areas in parent and non-FKD cell sheets decreased notably due to the cell migration, however, the mean scratch area in FKD cell sheets decreased only slightly (Fig. 4A and B). FKD cell migration showed a statistical difference from parent and non-FKD cells (Tukey-Kramer test, $P<0.01$).

In 2D LV-SEM observation, non-FKD cell sheet exhibited loose cell-cell connections (Fig. 5A), whereas the cells of FKD cell sheet were observed as groups with tight cell-cell connections (Fig. 5B). Bundles of extremely thin microfibrils (filopodia) existed on the surface of leading migratory non-FKD cells (Fig. 5C). By contrast, globular-shaped lamps of different sizes were observed on the surface of FKD cells (Fig. 5D).

Correlative light and electron microscopy (CLEM). Fascin expression (green; Fig. 6) was strongly positive in non-FKD cells, which exhibited thin filopodia on the cell membrane (arrows). Meanwhile, fascin expression was effectively suppressed in FKD cells, and globular-shaped lamps were observed on the cell membrane (arrowheads). In LV-SEM, numerous lamps were recognized as whitish spots on the surface of FKD cells (arrowheads). Thus, fascin-positive spots observed by optical microscope were demonstrated to locate at the whitish spots in the bulbous-shaped protrusions on the FKD cell surface in LV-SEM.

HE and immunohistochemical study. Non-FKD and FKD cells were cultured in Cellmatrix® for 10 days. Following HE staining, non-FKD cells were observed to have loose cell-cell adhesions, whereas clusters with cell-cell connections were observed in FKD cells (Fig. 7). E-cadherin

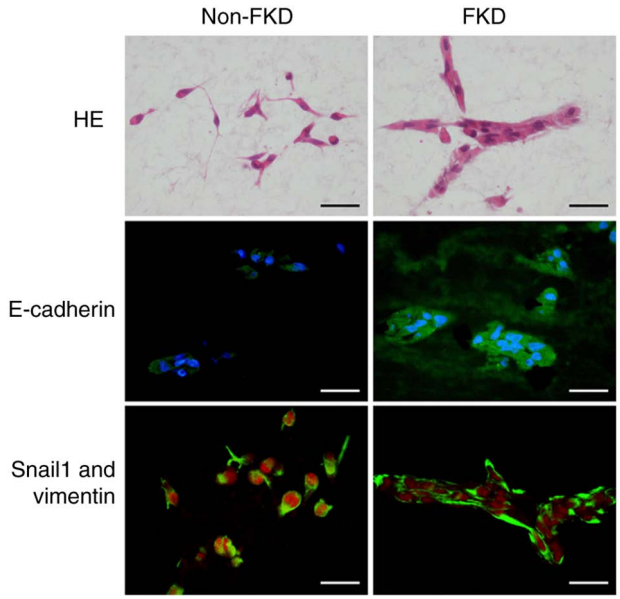

Figure 7. HE and immunohistochemical staining of non-FKD and FKD MDA-MB-231 cells cultured in Cellmatrix®. HE staining showed non-FKD cells with loose cell-cell connections, whereas FKD cell adhesion formed clusters. E-cadherin (green) immunohistochemical staining was negative in non-FKD cells but positive in FKD cells. The cell nucleus was stained in blue by DAPI. Snail1 expression (red) was notably higher in the cell nucleus of non-FKD cells compared with FKD cells. Vimentin (green) was strongly positive in both non-FKD and FKD cells. Scale bar, 50 μm. HE, hematoxylin-eosin; FKD, fascin knockdown.

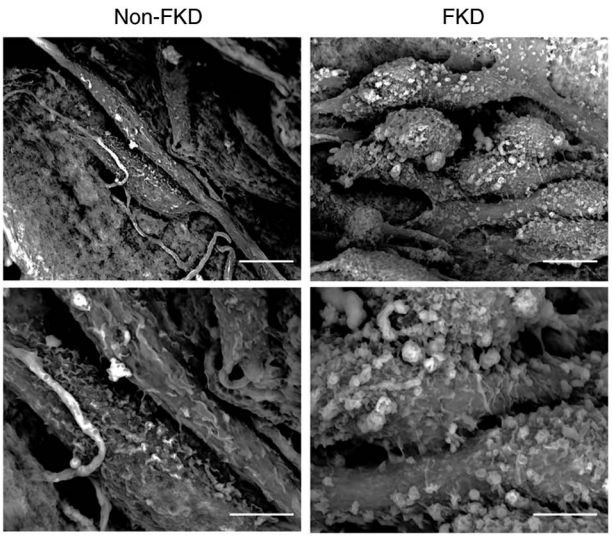

Figure 8. Three-dimensional low vacuum-scanning electron microscopy of non-FKD and FKD MDA-MB-231 cells cultured in Cellmatrix®. Numerous thin protrusions (filopodia) were observed on the surface of non-FKD cells, and cells exhibited loose cell-cell adhesion. Bulbous-shaped protrusions of varied sizes were observed on the surface of FKD cells, which exhibited partial cell-cell adhesion. Scale bar, upper pictures: 10 μm, lower pictures: 5 μm. FKD, fascin knockdown.

immunohistochemical staining was negative in non-FKD cells but positive in FKD cells. Snail1 expression (red) was observed in the nucleus of non-FKD cells but was decreased in FKD cells; however, vimentin was strongly positive in both cell lines (green). E-cadherin expression was significantly

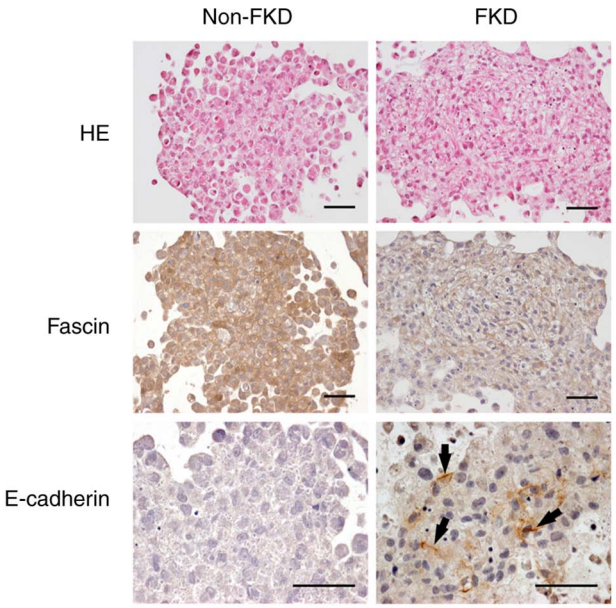

Figure 9. HE and immunohistochemistry staining of non-FKD and FKD MDA-MB-231 cell spheroids cultured in Cellmatrix®. Densely aggregated tumor cells with irregularly shaped nuclei were observed in both non-FKD and FKD cell spheroids. Fascin expression was strongly positive in non-FKD spheroid. Arrows indicate E-cadherin-positive membrane staining. Scale bar, 50 μm. HE, hematoxylin-eosin; FKD, fascin knockdown.

different between non-FKD and FKD cells, and Snail1 expression as well ($P<0.01$).

3D LV-SEM observation. Numerous thin cell protrusions (filopodia) were observed on the surface of non-FKD cells (Fig. 8). These cells exhibited loose cell-cell adhesions. By contrast, bulbous-shaped protrusions of varied sizes were detected on the surface of FKD cells, which exhibited partial cell-cell adhesions.

Spheroid cell culture. Densely aggregated tumor cells with irregularly shaped nuclei were observed in both non-FKD and FKD cells (Fig. 9). Fascin expression was strongly positive in non-FKD cells. Arrows indicate E-cadherin positive-stained membranes observed in FKD cells.

In 3D LV-SEM observation, non-FKD spheroid cells gathered densely forming a spherical spheroid block, by contrast, cells of the FKD spheroid gathered sporadically and eventually formed an irregularly shaped spheroid block (Fig. 10). There were numerous cell protrusions (filopodia) on the surface of non-FKD spheroid cells, in contrast, globular-shaped protrusions of varied sizes were observed on the surface of FKD spheroid cells. The morphological appearances of parent cells were similar to non-FKD cells.

In stereoscopic microscope observation, homogeneous filamentous cells were observed infiltrating into the surrounding gel from the non-FKD spheroid (Fig. 11A), while irregular heterogeneous fascicular cell invasion into the gel was observed from the FKD spheroid (Fig. 11B). HE staining revealed fibrous spindle-shaped tumor cells invading the surrounding gel from the non-FKD spheroid (Fig. 11C), while clusters of tumor cells (arrows; Fig. 11D) originating from the FKD spheroid were observed invading the gel.

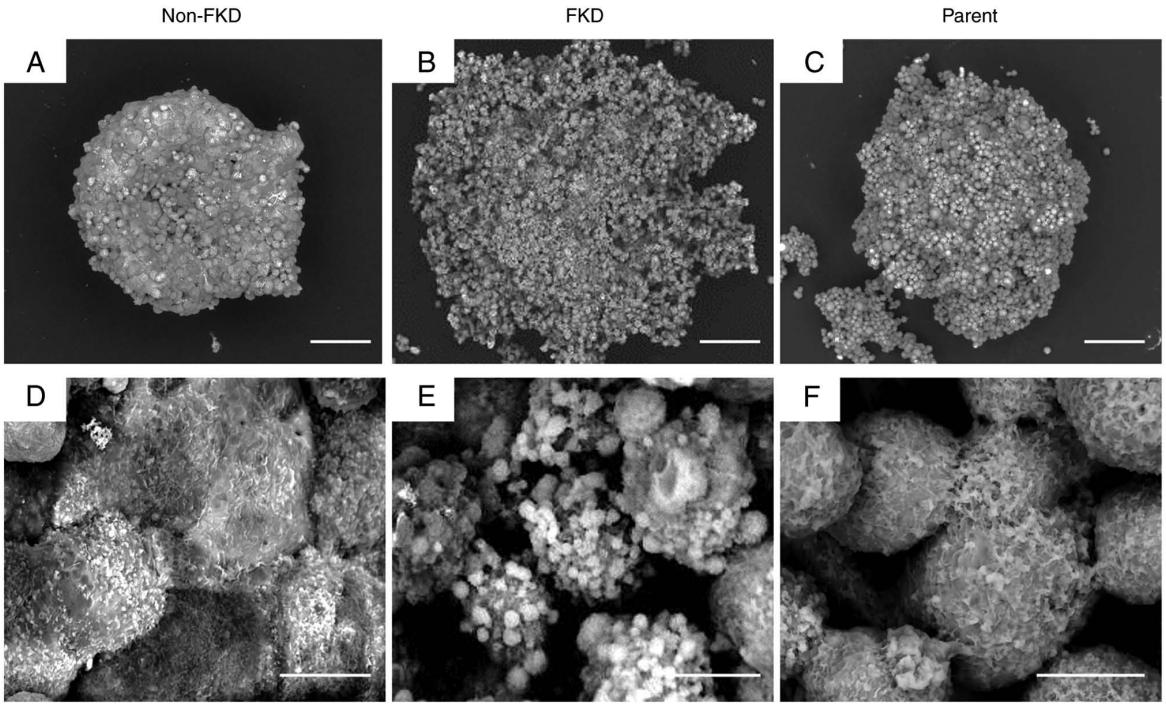

Figure 10. Three-dimensional low vacuum-scanning electron microscopy of non-FKD, FKD and parent MDA-MB-231 cell spheroids cultivated. Cells of non-FKD spheroid were observed to gather densely forming a spherical spheroid block and globular-shaped protrusions of varied sizes were observed on the surface of FKD spheroid cells (A, D). FKD spheroid cells gathered with loose cell-cell connections and formed an irregularly shaped spheroid block (B, E). Numerous cell protrusions (filopodia) on the surface of non-FKD spheroid cells (D). The morphological appearances of parent cells were similar to non-FKD cell (C, F). Scale bar, upper pictures: 100 μm, lower pictures: 10 μm. FKD, fascin knockdown.

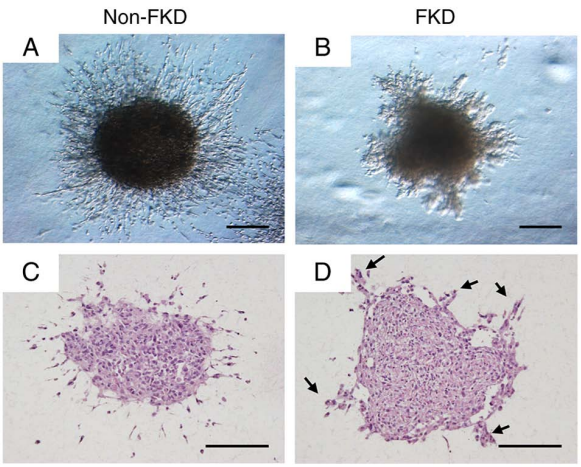

Figure 11. Representative cell invasion of non-FKD and FKD MDA-MB-231 spheroids cultured in Cellmatrix®. Stereoscopic images of non-FKD and FKD cell spheroids, cultivated in Cellmatrix for 3 days after cell seeding. (A) Homogeneous filamentous cells were observed infiltrating the surrounding gel from non-FKD spheroid. (B) Irregular heterogeneous fascicular cell invasion into the gel was observed from FKD spheroid. (C) Hematoxylin-eosin staining showed fibrous spindle-shaped tumor cells invading the surrounding gel from non-FKD spheroid. (D) Migration of tumor cell clusters (arrows) originating from FKD spheroid to the gel was observed. Scale bar, 500 μm. FKD, fascin knockdown.

Discussion

BC is the most frequently diagnosed cancer in female patients. Treatment of BC has improved, however the mortality of BC remains high among cancer-associated death in female patients (1-3). In the present study, during 5-year follow-ups, metastasis or recurrence occurred in 11 out of 100 consecutive Japanese patients diagnosed with early-stage BC at Kochi University Hospital, Japan, in 2015. In the United States, similarly, it is reported that nearly 12% of patients with BC develop metastasis or recurrence (19). However, rising rates of BC incidence and mortality in underdeveloped countries have been reported (1,20). Different factors, such as diet, alcohol, smoking, contraceptive pills and physical exercise may affect prognosis of BC (2). When BC is detected and treated at the earlier stages, more favorable prognosis can be achieved, as with other types of cancer (3,21).

Fascin is an actin-bundling protein. Fascin composes filopodia, slender bundled actin containing plasma membrane protrusions, which serve an important role in cellular processes such as cell adhesion, migration, wound healing, and the formation of cell-cell contacts by stimulating migration at the leading edge of cells (22,23). Recent studies have shown that fascin also localizes to invadopodia, actin-rich protrusions of the plasma membrane at the adherent cell surface, which facilitate extracellular matrix invasion (24,25). Lamb and Tootle (23) suggested that fascin may serve multiple functions to control cell migration; decreased fascin and prostaglandin expression induces delayed migration of border cells and elongated cell clusters (26). Higher fascin expression is associated with poorer prognosis in numerous types of cancer and sarcoma. Thus, fascin is considered to be key for cancer progression (7,10,13,16,17). The present study investigated the association between fascin and BC cell invasion via morphological observation of the cytoplasm and the cell surface. Previous studies have investigated the mechanism of how fascin increases cell migration and invasiveness to uncover

an effective treatment for malignant tumors, including BC, by targeting fascin (17,27,28). Accordingly, at the annual meeting of the American Society of Clinical Oncology, 2021, Novita Pharmaceuticals presented Phase 1A results of fascin inhibitor NP-G2-044 in patients with advanced and metastatic solid tumor, which was shown to be safe and effective (29).

Despite advances in research, diagnosis and treatment of BC, TNBC is an aggressive subtype with a high rate of metastasis or recurrence (1,6,7). Esnakula *et al* (7) confirmed a strong association between TNBC and fascin. Wang *et al* (10) suggested that fascin may be used as a novel diagnostic marker of TNBC. The present results similarly suggested that fascin may serve as an index to evaluate malignancy of early-stage BC and there was a significant association between TNBC subtype and the incidence of metastasis or recurrence. Patients who developed metastasis with negative or slightly positive fascin expression were also included in the present study. Hence, to examine how TNBC cells migrate following down-regulation of fascin, the present study established FKD and non-FKD MDA-MB-231 cells and performed wound healing assay, spheroid cell cultures, and 2D and 3D LV-SEM.

MDA-MB-231, a cell line isolated from a patient with invasive ductal BC, is characterized by negative ER, PR and E-cadherin expression and p53 mutation (30). The cells also lack growth factor receptor HER2 and represent a good model of TNBC (30). Hoa *et al* (31) knocked down fascin in human U251 glioma cells and confirmed that these cells lost microvilli and altered the glioma morphology. The present study successfully established FKD and non-FKD TNBC cells using MDA-MB-231.

The wound healing assay may be performed under various circumstances, such as mechanical, thermal or chemical damage, however, it is a 2D approach and its utility is limited to the observation of cells migrating as a collective epithelial sheet (32). Therefore, the wound healing assay does not simulate the natural environment where cells exist with cell-cell and cell-extracellular matrix interactions. A more ideal *in vitro* cell model that facilitates observation of migration of malignant cells is 3D spheroid cell culture. Compared with 2D monolayer culture, such as wound healing assay, spheroid cell cultures more accurately reflect the microenvironment *in vivo* (32).

LV-SEM in the present study demonstrated that FKD morphologically modified the surface of TNBC cells. When fascin was knocked down, cells lost filopodia, which are key for cell migration into the surrounding microenvironment. FKD cells developed granular lamps of various sizes that facilitated cell-cell connection. The spheroid culture showed that following FKD, tumor cells developed clusters and migrated into the surrounding gel. Fox *et al* (26) demonstrated that fascin promotes single cell migration; the present findings suggested that suppression of fascin induced collective migration of TNBC cells. The wound healing assay indicated that cell migration ability was impaired due to FKD, however, 3D spheroid cell culture suggested that modification of the surface of tumor cells facilitated collective cell migration. These results indicated that TNBC cells maintained the ability to migrate following FKD via collective cell migration.

Cancer metastasis is a radical progression of malignant cells that migrate into the surrounding microenvironment and its mechanism is generally classified as single or collective cell migration (15,33). Single cell migration has been studied widely, primarily using 2D cell cultivation methods that do not reflect the *in vivo* environment (33-36). The theory of collective cell migration is relatively new. 3D methods, such as a spheroid cell culture used in the present study, facilitate analysis of collective cell migration, which is considered to be a primary mechanism of cancer metastasis (33-36). However, cell migration process does not occur only at the single focal adhesion level, but it is also affected by the integration with surrounding cells (36). Thus, it is indispensable to observe the mechanism of different migration patterns. The present study performed the classic 2D wound healing assay and modern 3D spheroid cell culture, which indicated that MDA-MB-231 cells exhibited collective migration following FKD.

Certain patients did not develop metastasis or recurrence despite strong positive fascin expression. The Allred scores of Cases #14 and #22 were 6 and 8, respectively. These patients may have exhibited more favorable prognosis because the cancer subtype was not TNBC. These patients had detected breast tumors by self-exam, had an immediate consultation with a specialist and underwent surgery within two months of self-exam. Regular breast self-exam can detect cancer at an early stage, allowing more effective and less invasive treatment and leading to a more favorable prognosis (3,21).

The present study performed CLEM, one of the most advanced methods to observe cells morphologically and understand the dynamics of organelles. Recently, CLEM has achieved insights into cell biology by making it possible to observe the same area as an optical microscope with an electron microscope (37-39). Here, CLEM demonstrated fascin-positive spots observed by optical microscope located at the whitish spots in the bulbous-shaped protrusions on the FKD cell surface in LV-SEM.

The present study demonstrated collective migration of TNBC cells by 3D LV-SEM. TNBC cells may migrate into the surrounding microenvironment through collective migration in FKD cells that lack filopodia on the cell surface.

Acknowledgements

The authors would like to thank Dr Nobuaki Yamanaka, Dr Kazuho Honda, and Mr. Takeshi Kamimura (The LVSEM Study Group of Renal Biopsy, Tokyo, Japan) for technical assistance of the LVSEM equipment.

Funding

The present study was supported by grant research No. 006 of the LVSEM Study Group of Renal Biopsy from the LVSEM Study Group of Renal Biopsy and Hitachi High-Tech.

Availability of data and materials

The datasets used and/or analyzed during the current study are available from the corresponding author on reasonable request.

Authors' contributions

YY and YH conceived the study and performed experiments. YH and IM evaluated Allred score of fascin expression. YY

and HS performed statistical analysis. YY wrote the manuscript. IM supervised the study. YY and YH confirm the authenticity of all the raw data. All authors have read and approved the final manuscript.

Ethics approval and consent to participate

The present study was reviewed and approved by the Ethic Committee for Clinical Research of the School of Medicine, Kochi University (approval no. 2020-123). Written consent to participate was obtained from all patients.

Patient consent for publication

Not applicable.

Competing interests

The authors declare that they have no competing interests.

References

1. Fahad Ullah M: Breast cancer: Current perspectives on the disease status. Adv Exp Med Biol 1152: 51-64, 2019.
2. Coughlin SS: Epidemiology of breast cancer in women. Adv Exp Med Biol 1152: 9-29, 2019.
3. DeSantis CE, Bray F, Ferlay J, Lortet-Tieulent J, Anderson BO and Jemal A: International variation in female breast cancer incidence and mortality rates. Cancer Epidemiol Biomarkers Prev 24: 1495-1506, 2015.
4. Cancer Statistics. Cancer Information Service, National Cancer Center, Japan (National Cancer Registry, Ministry of Health, Labour and Welfare). https://ganjoho.jp/public/index.html.
5. Katanoda K, Ito Y and Sobue T: International comparison of trends in cancer mortality: Japan has fallen behind in screening-related cancers. Jpn J Clin Oncol 51: 1680-1686, 2021.
6. Grayson M: Breast cancer. Nature 485: S49, 2012.
7. Esnakula AK, Ricks-Santi L, Kwagyan J, Kanaan YM, DeWitty RL, Wilson LL, Gold B, Frederick WA and Naab TJ: Strong association of fascin expression with triple negative breast cancer and basal-like phenotype in African-American women. J Clin Pathol 67: 153-160, 2014.
8. Yamamoto Y, Hayashi Y, Sakaki H and Murakami I: Fascin-1 is associated with recurrence in solitary fibrous tumor/hemangiopericytoma. Mol Clin Oncol 15: 199, 2021.
9. Hayashi Y, Osanai M and Lee GH: Fascin-1 expression correlates with repression of E-cadherin expression in hepatocellular carcinoma cells and augments their invasiveness in combination with matrix metalloproteinases. Cancer Sci 102: 1228-1235, 2011.
10. Wang CQ, Tang CH, Chang HT, Li XN, Zhao YM, Su CM, Hu GN, Zhang T, Sun XX, Zeng Y, *et al*: Fascin-1 as a novel diagnostic marker of triple-negative breast cancer. Cancer Med 5: 1983-1988, 2016.
11. Arlt MJ, Kuzmanov A, Snedeker JG, Fuchs B, Silvan U and Sabile AA: Fascin-1 enhances experimental osteosarcoma tumor formation and metastasis and is related to poor patient outcome. BMC Cancer 19: 83, 2019.
12. Richmond AM, Blake EA, Torkko K, Smith EE, Spillman MA and Post MD: Fascin is associated with aggressive behavior and poor outcome in uterine carcinosarcoma. Int J Gynecol Cancer 27: 1895-1903, 2017.
13. Allred DC, Harvey JM, Berardo M and Clark GM: Prognostic and predictive factors in breast cancer by immunohistochemical analysis. Mod Pathol 11: 155-168, 1998.
14. Yamamoto Y, Hayashi Y, Sakaki H and Murakami I: Evaluation of clinical and immunohistochemical factors relating to melanoma metastasis: Potential roles of nestin and fascin in melanoma. Diagnostics (Basel) 12: 219, 2022.
15. Lamb MC, Kaluarachchi CP, Lansakara TI, Mellentine SQ, Lan Y, Tivanski AV and Tootle TL: Fascin limits Myosin activity within Drosophila border cells to control substrate stiffness and promote migration. Elife 10: e69836, 2021.
16. Abbasi A, Noroozinia F, Anvar S, Abbasi M, Hosseinzadeh S and Mokhtari S: Fascin overexpression is associated with higher grades of breast cancer. Pol J Pathol 70: 264-268, 2019.
17. Xing P, Li JG, Jin F, Zhao TT, Liu Q, Dong HT and Wei XL: Fascin, an actin-bundling protein, promotes breast cancer progression in vitro. Cell Biochem Funct 29: 303-310, 2011.
18. Arjonen A, Kaukonen R and Ivaska J: Filopodia and adhesion in cancer cell motility. Cell Adh Migr 5: 421-430, 2011.
19. Peart O: Metastatic breast cancer. Radiol Technol 88: 519M-539M, 2017.
20. Iqbal J, Ginsburg O, Rochon PA, Sun P and Narod SA: Differences in breast cancer stage at diagnosis and cancer-specific survival by race and ethnicity in the United States. JAMA 313: 165-173, 2015.
21. Ginsburg O, Yip CH, Brooks A, Cabanes A, Caleffi M, Dunstan Yataco JA, Gyawali B, McCormack V, McLaughlin de Anderson M, Mehrotra R, *et al*: Breast cancer early detection: A phased approach to implementation. Cancer 126 (Suppl 10): S2379-S2393, 2020.
22. Mattila PK and Lappalainen P: Filopodia: Molecular architecture and cellular functions. Nat Rev Mol Cell Biol 9: 446-454, 2008.
23. Lamb MC and Tootle TL: Fascin in cell migration: more than an actin bundling protein. Biology (Basel) 9: 403, 2020.
24. Lin S, Li Y, Wang D, Huang C, Marino D, Bollt O, Wu C, Taylor MD, Li W, DeNicola GM, *et al*: Fascin promotes lung cancer growth and metastasis by enhancing glycolysis and PFKFB3 expression. Cancer Lett 518: 230-242, 2021.
25. Wang Y, Song M, Liu M, Zhang G, Zhang X, Li MO, Ma X, Zhang JJ and Huang XY: Fascin inhibitor increases intratumoral dendritic cell activation and anti-cancer immunity. Cell Rep 35: 108948, 2021.
26. Fox EF, Lamb MC, Mellentine SQ and Tootle TL: Prostaglandins regulate invasive, collective border cell migration. Mol Biol Cell 31: 1584-1594, 2020.
27. Lin S, Taylor MD, Singh PK and Yang S: How does fascin promote cancer metastasis? FEBS J 288: 1434-1446, 2021.
28. Ristic B, Kopel J, Sherazi SAA, Gupta S, Sachdeva S, Bansal P, Ali A, Perisetti A and Goyal H: Emerging role of fascin-1 in the pathogenesis, diagnosis, and treatment of the gastrointestinal cancers. Cancers (Basel) 13: 2536, 2021.
29. Chung V, Jhaveri KL, Van Hoff DD Von, Huang XY, Garmey EG, Zhang J and Tsai FYC: Phase 1A clinical trial of the first-in-class fascin inhibitor NP-G2-044 evaluating safety and anti-tumor activity in patients with advanced and metastatic solid tumors. J Clin Oncol 39 (15 Suppl): S2548, 2021.
30. JoEllen W: Chapter 40 - Animal Models for Studying Prevention and Treatment of Breast Cancer. In: Animal Models for the Study of Human Disease. Elsevier, Amsterdam, pp997-1018, 2013.
31. Hoa NT, Ge L, Erickson KL, Kruse CA, Cornforth AN, Kuznetsov Y, McPherson A, Martini F and Jadus MR: Fascin-1 knock-down of human glioma cells reduces their microvilli/filopodia while improving their susceptibility to lymphocyte-mediated cytotoxicity. Am J Trransl Rransl Res 7: 271-284, 2015.
32. Huang Z, Yu P and Tang J: Characterization of triple-negative breast cancer MDA-MB-231 cell spheroid model. Onco Targets Ther 13: 5395-5405, 2020.
33. Trepat X, Chen Z and Jacobson K: Cell migration. Compr Physiol 2: 2369-2392, 2012.
34. Lamb MC, Anliker KK and Tootle TL: Fascin regulates protrusions and delamination to mediate invasive, collective cell migration in vivo. Dev Dyn 249: 961-982, 2020.
35. Lintz M, Muñoz A and Reinhart-King CA: The mechanics of single cell and collective migration of tumor cells. J Biomech Eng 139: 0210051-0210059, 2017.
36. De Pascalis C and Etienne-Manneville S: Single and collective cell migration: The mechanics of adhesions. Mol Biol Cell 28: 1833-1846, 2017.
37. Sanada T, Yamaguchi J, Furuta Y, Kakuta S, Tanida I and Uchiyama Y: In-resin CLEM of Epon-embedded cells using proximity labeling. Sci Rep 12: 11130, 2022.
38. Peng D, Li N, He W, Drasbek KR, Xu T, Zhang M and Xu P: Improved fluorescent proteins for dual-colour post-embedding CLEM. Cells 11: 1077, 2022.
39. Van den Dries K, Fransen J and Cambi A: Fluorescence CLEM in biology: Historic developments and current super-resolution applications. FEBP Lett 596: 2486-2496, 2022.